Catalysis Today 178 (2011) 34–41

Contents lists available at SciVerse ScienceDirect

Catalysis Today

journal homepage: www.elsevier.com/locate/cattod

Process design and performance of a microstructured convective steam–methane reformer

Brian S. Haynes[a,*], Anthony M. Johnston[b]

[a] School of Chemical and Biomolecular Engineering, University of Sydney, NSW 2006, Australia
[b] Optint Pty Ltd., Level 5, Edgecliff Centre, Edgecliff, NSW 2027, Australia

ARTICLE INFO

Article history:
Received 2 June 2011
Received in revised form 27 August 2011
Accepted 29 August 2011
Available online 12 October 2011

Keywords:
Printed circuit heat exchanger
Process integration
Scalability
Autoregulation

ABSTRACT

We describe the design and operation of a microstructured steam–methane reformer in which the heat transfer area and reaction volume demands for the reforming process are decoupled to yield a high degree of process intensification relative to conventional tubular reformer design. The plant design incorporates intensive process integration without steam export. With 80% hydrogen recovery from the syngas in a PSA, and use of the PSA offgas as the only fuel source, the reformer system has a fuel energy efficiency of 78.6% as designed, corresponding to a hydrogen production rate of 2.69 mol H_2 per mol NG.

Based on printed-circuit heat exchanger techniques, the demonstration plant incorporates 17 stages of reforming at nominally 15 bar. Heating for the individual adiabatic stages is provided by combustion stages and by flue-gas heat recovery. The plant incorporates design features to minimise potential for carbon deposition and metal dusting. It displays intrinsic autoregulation over a wide range of turn-down, from 34% to 125%. Start-up is very rapid, approximately 2 h from cold to syngas production at full rate.

With these features, this process and plant design is well suited for standalone operation, for example to substitute for merchant hydrogen delivery in small or isolated facilities. While the present plant has a capacity of 5 Nm^3 H_2 h^{-1}, the multichannel printed circuit architecture is scalable without loss of precision to very large throughputs.

1. Introduction

David Trimm had a special relationship with reforming, at least of methane if not of his waggishness, which was irrepressible. From his early work on partial oxidation [1], through his authoritative studies of coke formation [2,3], and on to small scale reformers for on-board fuel processing [4] and remote installations [5], his work was for 40 years a spotlight on what was scientifically and technically important in the area. This paper links into Trimm's interest in small-scale reforming systems.

In previous publications [6–8], we described the design and demonstration of a scalable, microstructured steam methane reformer. That system operated at 2 bar and was conceived primarily as a primary fuel processor for a hydrogen fuel cell. This paper reports on a revised SMR process that operates at 15 bar. At this pressure, the hydrogen can readily be purified by pressure-swing absorption to provide a very pure hydrogen stream suitable for fuel cells and the many industrial applications that are currently serviced by a merchant hydrogen supply. Alternatively, the syngas can be used in further downstream processing.

Rostrup-Nielsen [9] has summarised the current and developing status of steam–methane reforming plant for syngas production. Current practice is generally to react natural gas with steam over a nickel catalyst in large tubular reformers operating at temperatures in excess of 800 °C. The catalyst is extremely active and the rate of heat transfer limits the reaction intensity that can be achieved. In large scale equipment, high heat fluxes are attainable using high-temperature radiant transfer – the tubes containing the catalyst are located within a fired furnace, with heat transfer being almost entirely by radiation from the flame and combustion gases, as well as from the walls. The high temperatures needed to obtain high radiant heat fluxes (typical design heat fluxes being of the order of $q \sim 100\,kW\,m^{-2}$) mean that the combustion gases leave the furnace at around 900 °C – heat is recovered in a waste heat boiler but, with steam generated also from the hot combustion flue gases, the overall quantity of steam generated greatly exceeds the reformer process requirements and excess steam is exported for use elsewhere, for example for compression of the reactor feed to a downstream ammonia plant. Credit is generally taken for this export steam when the efficiency of a reformer process is being assessed. However, there are applications where the excess steam really has very little value because of a lack of opportunities to exploit it. In these situations, the radiant reformer really does not perform very well in terms of its intrinsic thermal efficiency.

* Corresponding author. Tel.: +61 2 9351 3435.
E-mail address: brian.haynes@sydney.edu.au (B.S. Haynes).

0920-5861/$ – see front matter © 2011 Elsevier B.V. All rights reserved.
doi:10.1016/j.cattod.2011.08.048

In particular, if the objective of the reforming produce is to manufacture hydrogen as a final product, surplus steam is often problematical. A reduction in the steam–carbon ratio in the reformer helps reduce the magnitude of the problem, but at the risk of exacerbating the propensity to form carbon in the system. Therefore, the manufacture of hydrogen is sometimes carried out in a convective reformer in which heat exchange from the hot exhaust streams (flue gas and products) supplies energy for the reforming process.

We consider here a simple demonstration of the heat fluxes achievable with convective reforming. For heat transfer from atmospheric-pressure combustion gases, the dominant resistance to heat transfer is from the combustion gases to the wall. For flow across a bundle of tubes (containing the catalyst, diameter typically of the order of 100 mm), the external heat transfer coefficient may be estimated very crudely via Colburn's correlation

$$Nu = 0.33 Re^{0.6} Pr^{0.33}$$

Here the Reynolds number is based on the velocity occurring in the minimum open area between the tubes – a typical value would be 20 m s^{-1}. Taking physical properties for combustion flue gases at 1 bar and 900 °C, we obtain a heat transfer coefficient of $h \sim 70\,\mathrm{W\,m^{-2}\,K^{-1}}$ which in turn would require an infeasible temperature driving force ~1400 K in order to achieve a wall heat flux of $q = 100\,\mathrm{kW\,m^{-2}}$. In practice, of course, much lower temperatures and heat fluxes must be accepted, despite which the convective reformer does still offer some volume reduction relative to a radiant furnace [9]. Nevertheless, the radiant furnace has remained the preferred plant for large-scale steam reforming.

Recent developments in process intensification have taken advantage of the fact that heat transfer rates are greatly enhanced in smaller-scale systems and a number of convective reformer concepts have been advanced and demonstrated. In parallel plate reformers, the combustion and reforming processes take place in adjacent channels, creating a heat-exchanger/reactor with the channel wall providing both the support for catalysts that promote the respective processes and the heat transfer dividing wall. Because of the narrow channel width employed, the flows in these systems are typically laminar, for which a characteristic Nusselt number is easily obtained as a constant value under fully developed conditions. For a flat-plate arrangement, this value is

$$Nu \sim 8$$

For a typical plate separation of 1 mm ($d_h = 2$ mm), the corresponding heat transfer coefficient for flue gases is $h \sim 320\,\mathrm{W\,m^{-2}\,K^{-1}}$ – now a heat flux of $100\,\mathrm{kW\,m^{-2}}$ can be achieved with a temperature driving force of just 320 K, which is not far removed from what is achievable with radiation in a large-scale furnace. However, the large exchange area per unit volume that is achievable with separation distance of the order of 1 mm compared with the scale of perhaps 100 mm in a conventional convective reformer (or some metres in a radiant firebox) means that these "microstructured" devices are very much smaller [10].

It is possible to augment the heat transfer in laminar flow by a number of techniques. Passages shorter than the thermal development length enjoy the benefits of thinner boundary layers and higher heat transfer coefficients. When fluids pass through a curved duct, secondary flows (Dean vortices) are developed which promote the transverse mixing of the fluid in the duct and so enhance the heat transfer rate. At sharp bends, recirculation zones may be established, also leading to mixing of the fluid at that point – beyond the bend the laminar boundary layer must re-establish, during which process significantly higher (developing flow) heat transfer coefficients are obtained. Significant augmentation is possible using a combination of the above techniques, meaning that the nominal reformer heat flux of $100\,\mathrm{kW\,m^{-2}}$ can be achieved with a temperature driving force <100 K for flow in 1 mm passages. Applied to the reforming example, this in turn allows one to think in terms of processes with close temperature approaches and very high thermal efficiency.

Even smaller driving forces can be achieved if the duct diameter is reduced further. However, there is a limit to how small passage dimensions should go. In general terms, finer passages must be made shorter and used in larger numbers in order to control the pressure drop in a given duty; furthermore, from the point of view of manufacturing, the attachment of flow headers and distribution systems to very short arrays of ducts becomes problematical; and very fine passages bring an increased risk of channel blockage.

There have been a very large number of publications on microreactor concepts for steam reforming published in the past decade. Unfortunately, in the vast majority of these publications, little or no attention is paid to the overall integration of the process from cold reactants to cooled products, the main foci being on the reaction kinetics of novel supported catalysts and on the configuration of the high-temperature heat supply (combustion) and heat sink (reforming) reactions.

In particular, a number of heat-exchanger/reactor concepts for steam reforming have been proposed and demonstrated [10–13] – Ref. [13] in particular provides a comprehensive survey of developments in this area. However, the common wall in these systems still links the reaction rate inextricably to the heat-transfer rate, giving rise to the potential for stability problems to occur in operation as catalysts age and in scaling out [14]. Another novel approach to intensifying the reforming reaction is to employ a hydrogen-selective membrane which removes the equilibrium limitations on the reformer conversion that become especially problematical at high pressures [15].

We have previously proposed [6] and demonstrated [7,8] a system of adiabatic reaction beds interleaved with heat exchangers as a means of separating the heat transfer area requirements from the reaction area. This approach allows each aspect (heat transfer and reaction) to be configured optimally for the task at hand and leads to profound levels of process integration. Integral to our multiple-adiabatic bed (MAB) approach was a very high thermal efficiency (with no steam export), minimal process control, excellent turn-down performance, and a high degree of scalability.

In this paper, we describe significant process improvements towards the further development of the MAB process for steam–methane reforming. We do not concern ourselves here with upstream or downstream processes such as gas compression, or syngas conversion to other products. Rather we focus on the microstructured process engineering of steam methane reforming as a highly efficient stand-alone process.

2. Process description and plant design

2.1. Process description

The overall process schematic is shown in Fig. 1 [16]. The reformer operates at 15 bar with a steam:carbon ratio of ~3.8. Combustor fuel and air are supplied at room temperature and close to atmospheric pressure (<1.3 bar). Liquid water and natural gas are supplied at room temperature at the operating pressure. The reformer catalyst is a commercial noble metal catalyst on a rippled metallic strip support; the combustion catalyst is a noble metal mixture on a monolith support.

Fig. 2 shows details of the multi-stage prereforming/reforming section. There are 3 stages of pre-reforming that initiate H_2 production under relatively mild conditions in order to inhibit carbon deposition at the higher temperatures of the main reformer stages. The incoming steam/methane mixture is heated in countercurrent

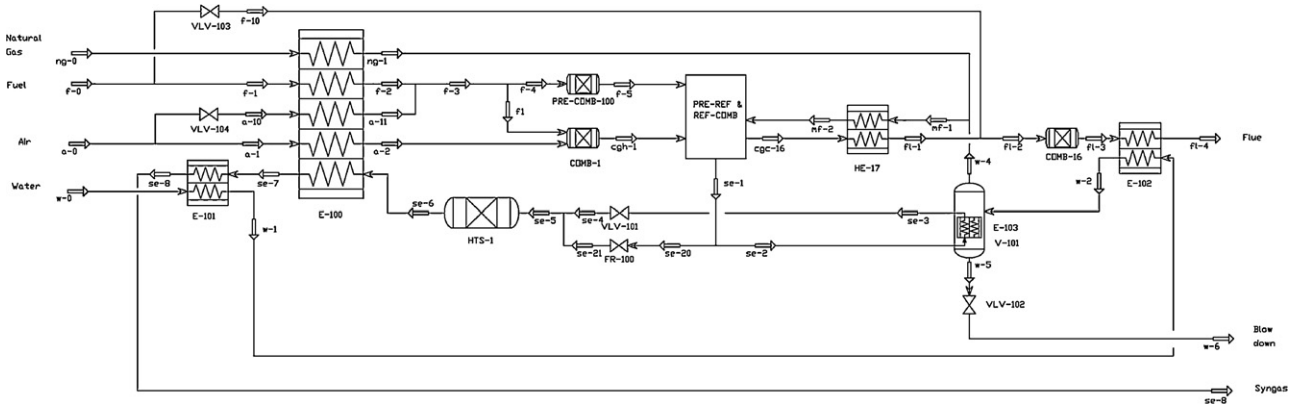

Fig. 1. Schematic diagram of the integrated SMR process. The pre-reformer/reformer/combustion block is shown in detail in Fig. 2.

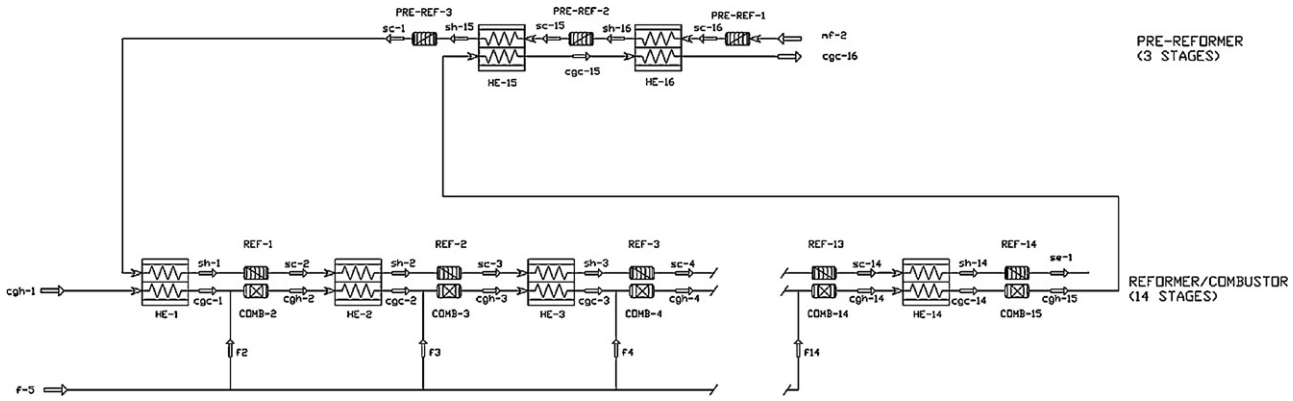

Fig. 2. Details of reaction stages showing interstage convective heating.

stagewise contact with the hot combustion flue gases, as shown in Fig. 2, to provide the reaction heat for the prereformers.

There are 14 stages in the main reforming block – after each stage, the partially reacted steam–methane mixture is reheated by heat exchange with hot combustion gases. The hot gases required at each stage are produced by catalytic combustion of fuel into the main combustion gas stream. The catalyst is based on noble metals supported on a ceramic monolith. This stream, initially air, is progressively vitiated through the stages until it leaves the last stage with a low residual oxygen content, typically <1% on a dry basis.

Fig. 3 depicts the sawtooth variation of reformer and combustion-side temperatures through the stages. By careful distribution of fuel to the successive combustion stages, the stagewise heat release is controlled, as is the stagewise inlet temperature and adiabatic conversion in the reformer stream. The reformer stream temperature is gradually increased through the process with the products leaving the final stage close to equilibrium at ~800 °C.

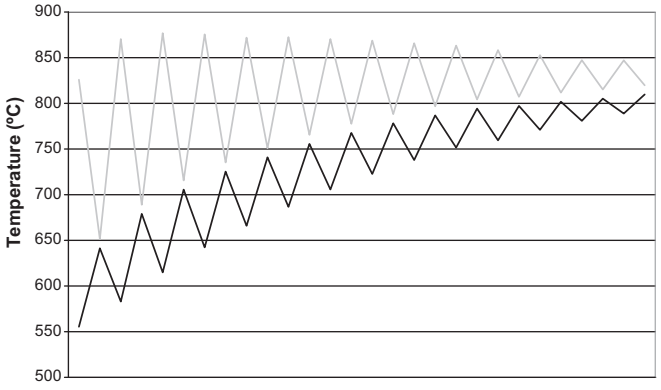

Fig. 3. Sawtooth temperature profiles for combustion (grey) and reformer (black) streams through the 14 stages of the multi-stage reformer.

There is intensive heat recovery from the hot combustion flue gas and reformer streams. Hot syngas generates steam (as described in more detail below) and enters the high-temperature shift reactor (HTS, using noble metal on monolith support) at about 300 °C. After picking up reaction heat in the HTS, the syngas then provides heat in a tightly integrated 5-stream exchanger to preheat the fuel, air, water and natural gas streams before leaving the process as a two-phase mixture. After providing heat for the performing stages, the flue gas is further cooled by contact with the partially preheated water stream.

Fig. 4 shows the grand composite curve for the process. The pinch point arises at the point where evaporation of water commences, around 200 °C, where the approach temperature is 34 °C. As a result of intensive heat recovery, the flue gas and syngas products leave at temperatures below 150 °C. Heat recovery extends to substantial condensation of the unconsumed steam remaining in the syngas but there are insufficient low-grade sinks within the process for complete condensation – some external cooling is therefore required to complete the condensation of this reagent steam. This cooling (not shown in Fig. 1) represents the only thermal utility required for operation of the plant.

2.2. Syngas cooling and steam generation

Syngas cooling is always challenging in reformers because of the potential for metal dusting. Metal dusting is a catastrophic carburisation phenomenon which occurs under conditions where the

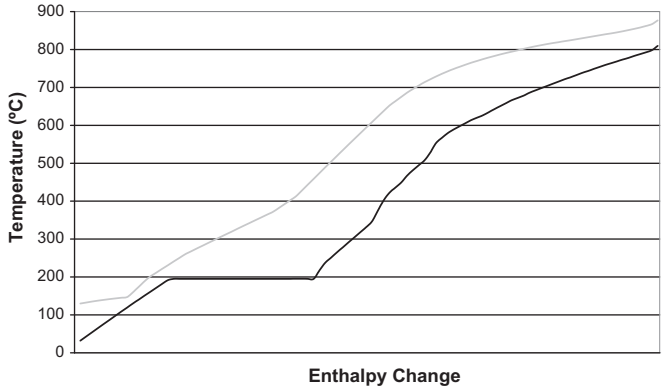

Fig. 4. Grand composite curve for the integrated reformer. The grey line corresponds to hot streams while the dark line corresponds to cold streams.

temperatures are in the approximate range 400–800 °C and the carbon activity of the gaseous atmosphere is greater than unity. Every effort is made in reformer operations to limit the zones in which syngas is prone to dusting, including even spraying water into the syngas in order to quench cool it. Depending on the need for steam beyond the SMR process, a more energy-efficient approach is to recover heat from the syngas in a process gas boiler in which the metal temperature is close to the saturation temperature of the steam being generated, at temperatures low enough for dusting to be too slow to be of concern in most applications, i.e. <400 °C.

In the present reformer, the issue of metal dusting in process heat recovery is managed by a combination of steam generation (just sufficient for the process) and dilution cooling using cooled syngas. A portion of the syngas is fed to the submerged-core steam generator in which the metal temperature is maintained close to the steam saturation temperature 200 °C. The syngas is itself cooled close to this temperature – there is a transition of metal temperature through the dusting regime at the syngas inlet to this exchanger and this short region is a protected by aluminide coating.

The cooled syngas leaving the boiler is then mixed with the remaining hot syngas so that the mixed temperature is low enough for dusting not to be of concern, in fact at the required inlet temperature for the HTS reactor, ~300 °C. The piping in the immediate vicinity of this mixing point is also coated for protection against dusting.

The steam/carbon ratio for the overall process is largely fixed by this arrangement, as a simple energy balance shows. If the preheated water stream entering the boiler has a thermodynamic steam quality $x|_{in}$:

$$\dot{m}_{syngas}\hat{C}_{p|syngas}(T_{reformer} - T_{HTS\ \ in}) = \dot{m}_{steam}\hat{\lambda}_{steam}(1 - x|_{in}) \quad (1)$$

With $\dot{m}_{syngas} = \dot{m}_{steam} + \dot{m}_{NG}$, and assuming the natural gas is essentially methane, this gives the S/C ratio

$$\mathrm{S/C} = \frac{16}{18}\frac{\dot{m}_{steam}}{\dot{m}_{NG}} = \frac{0.89}{((\hat{\lambda}_{steam}(1 - x|_{in}))/(\hat{C}_{p|syngas}(T_{reformer} - T_{HTS\ \ in}))) - 1} \quad (2)$$

For $x|_{in} \sim 0$, $T_{reformer}$ = 800 °C, $T_{HTS\,in}$ = 290 °C, and with typical values of $\hat{\lambda}_{steam} = 1950$ kJ kg^{-1} and $\hat{C}_{p|syngas} = 3.1$ kJ kg^{-1} K^{-1}, we obtain S/C ~ 3.8. It is noteworthy here that this ratio is intrinsic to the steady-state process and is not affected by turndown.

From the above equation, it can be seen that the intrinsic S/C ratio is affected by adjustments in the HTS inlet temperature. Such adjustments may need to be made (by altering the fraction of the hot syngas that goes to the boiler) to ensure that the HTS is operating optimally – for example if the inlet temperature is increased by 10 °C (to 300 °C), the S/C ratio becomes 3.4. Active control of the S/C ratio can be achieved by generating steam in the flue gas cooler (so that $x|_{in} > 0$) but we focus here on the simpler autoregulated operation that is particularly attractive for remote and distributed production.

2.3. Fuel distribution

Distribution of fuel into an MAB reformer needs careful management because, with microchannel construction, the network of distribution channels brings the fuel into close contact with hot metal. This is not a problem if the fuel is H_2 (such as in an anode off gas from a fuel cell), but use of hydrocarbon or syngas-derived fuel (such as purge gas produced with hydrogen purification in pressure-swing absorption) may bring attendant risks of channel blockage through coking and/or corrosion by metal dusting. This issue is addressed in the present system by premixing the fuel with air to create, after catalytic combustion, a very fuel-rich mixture that not only has a carbon activity low enough to preclude coking and metal dusting but is also hot enough to lie outside the region of concern for metal dusting. This mixture is the fuel that is then distributed to the downstream combustion stages in proportions that determine the temperature rise in each stage and the overall profile of temperatures through the reforming and combustion stages.

2.4. Design performance

There are diverse performance metrics that are utilised in evaluation of the performance of steam–methane reforming processes. Ultimately, it is the final use of the syngas that determines the relevance of any one metric. Of particular importance is the source of the fuel for the reformer – this may be fully imported or it may be derived entirely from the syngas itself, usually after some intermediate processing. For example, if hydrogen is separated from the syngas, then the residual syngas is available as a fuel; if the use of the syngas is methanol synthesis, then the tail-gas from the synthesis plant can contribute to the fuel load.

In the present process design, we hypothesised stand-alone operation of the reformer in conjunction with pressure-swing absorption to produce a pure hydrogen stream, with the PSA off-gases being returned in their entirety to the reformer as the only fuel for the reformer process. We define

$$\eta_{H_2} = \frac{\dot{n}_{H_2}^{export} LHV_{H_2}}{\dot{n}_{NG} LHV_{NG}}$$

where $\dot{n}$ is the (molar) flow and LHV is the lower heating value of the stream (on a molar basis): the superscript *export* signifies the net flow of pure hydrogen exported from the hypothetical PSA; *NG* refers to the natural gas feed to the reformer side. For reforming at 14 bar and 800 °C, $T_{HTS\,in}$ = 290 °C and with 80% H_2 recovery in the PSA, the operating point of the reformer as designed is S/C = 3.8 and with hydrogen fuel efficiency $\eta_{H_2} = 78.6\%$. This efficiency figure rises to 81.3% if an optimistic 90% H_2 recovery is assumed for the PSA. Reported values of fuel efficiency for steam reforming of methane to produce H_2 with additional fuel and without steam export range from 61% to 78% [17]. The detailed modelling work of Simpson and Lutz [18] has broadly similar conditions to ours (p = 10 bar, HTS inlet 300 °C, S/C = 3.2), utilising a membrane separator (90% recovery) to purify the hydrogen: for a balanced process (no additional fuel) with reformer temperature 700 °C, they report $\eta_{H_2} = 67\%$.

The ratio of molar or volumetric hydrogen production rate to methane consumptions is typically about 2.3 in large-scale steam reformers [19]. Our balanced process with 80% PSA efficiency reports a significantly higher value of 2.69 mol H_2 per mol NG.

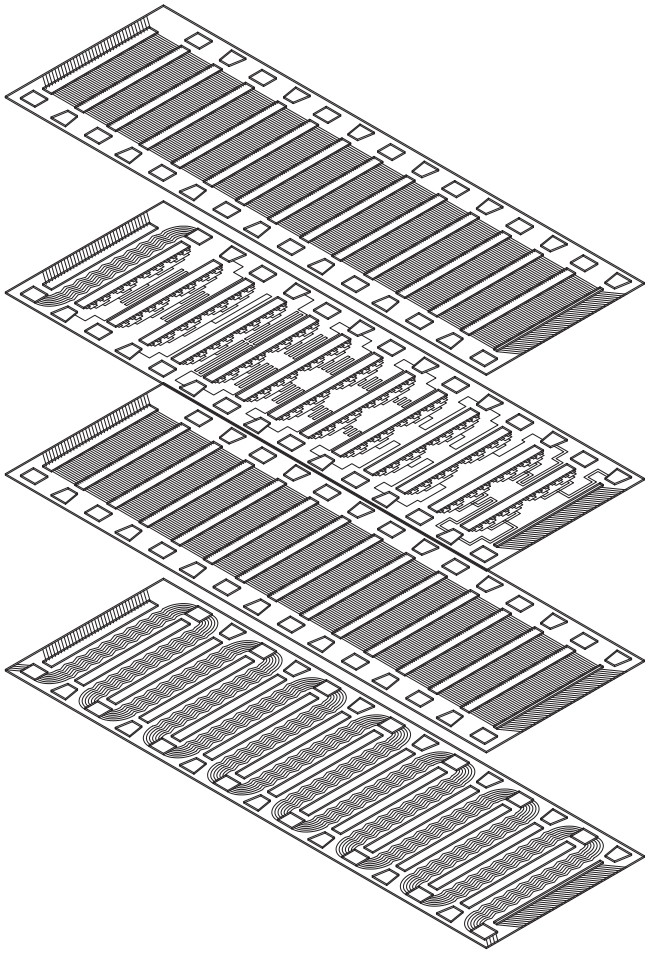

Fig. 5. Reformer plate etching and stacking arrangement. From the top down the plates are for (i) combustion air; (ii) fuel distribution; (iii) combustion air; and (iv) reforming. Overall flow direction in each plate is from right to left.

The very high values of these performance metrics for the present process are attributable to the high level of process integration incorporated in the design and represent a new benchmark for reformer performance.

2.5. Plant design and construction

The implementation of the process was designed to demonstrate the concept in a practical configuration using printed-circuit plate technology provided by Heatric (www.heatric.com). Fluid passages were etched into the metal plates, as shown schematically in Fig. 5 for the four plates comprising the repeating unit of the main reformer for which high-nickel alloy (800H) was employed. The first and third plates (from the top) carry the combustion air – the long slots crossing these plates are the openings for the catalyst chambers. These slots occur in all the plates to create the catalytic combustion chamber that extends through multiple repeating units but it is only the combustion gas plates and the fuel gas distribution plates (the second plate in Fig. 5 – see below) that have fluidic connection to these catalyst chambers. The fourth plate carries the reformer stream back and forth across the plate as it moves through the reforming reactor chambers located at the edges of the plate – in each pass across the plate, after exiting a reaction stage, this stream contacts the combustion stream and is reheated for further reaction in the next stage.

This distribution of fuel was achieved through the use of controlled fluidic resistances, as can be seen in the second plate in Fig. 5.

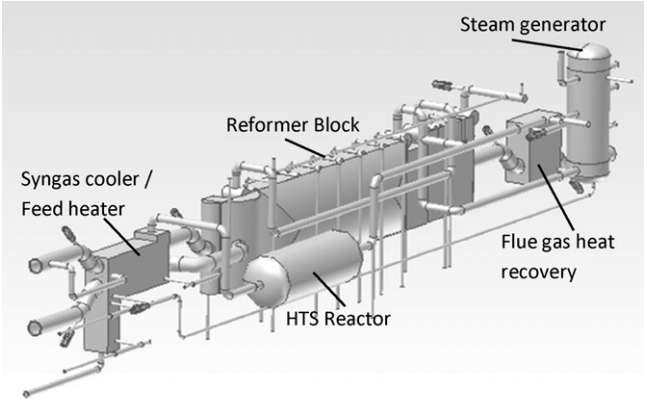

Fig. 6. Schematic of the assembled plant.

The flow in these channels is laminar to ensure that the relative resistances remain constant when the plant capacity is varied, thus ensuring passive fluidic control of this distribution.

This design is entirely scalable, with greater production rates entailing the use of more plates. For the purposes of demonstration, the production capacity was chosen to have enough repeating units to mitigate the effects of heat loss from the outer plates minimise edge effects which would otherwise disturb the intricate heat integration that the plant embodies. The nominal capacity of the present plant is 72 mol CH_4 h^{-1}. Assuming the natural gas is 100% CH_4 and ideal conversion to H_2, the plant capacity in terms of H_2 production is 288 mol h^{-1}, or 7 Nm^3 h^{-1} (298 K, 1 bar). The actual plant capacity was closer to 5 Nm^3 H_2 h^{-1} as a result of impurities in the natural gas, equilibrium limitations and catalyst performance.

The plate assemblies are diffusion-bonded together to form the three process blocks, prereformer and reformer, multistream feed effluent exchanger, and flue gas heat recovery unit, as shown in Fig. 6. The steam generator and HTS reactor are separate vessels that are coupled closely to the bonded blocks. The prereformer/reformer block is approximately 50 mm in thickness, 200 mm high an 1000 mm in length.

The whole system is insulated in high performance Microtherm insulation material (www.microtherm.uk.com).

3. Experimental

Operation of the system is carried out in a DCS environment (Yokogawa Quantum CS 3000) – this system provides alarms and interlocks for safe operation; it also enables comprehensive data logging. Sample for analysis of composition are taken at various points through the combustor and reformer chains. The samples are dried by water removal through selective membranes (Permapure driers) and analysed using calibrated microGC's (Varian 4900). Pressure drops are measured across many reaction and heat exchange elements. These arrangements are as described previously [7,8].

4. Results and discussion

The plant has operated for >1000 h in total, including 833 h during which natural gas was being introduced into the reformer, at steady state rates between 34% and 125% of the nominal production capacity of the plant. There have been 93 start-ups from cold – most runs were for short duration, typically 8 h of reforming but there have also been a number of 100-h tests.

The HTS catalyst installed in the system gradually deactivated under the conditions studied – an analysis of the performance of this catalyst will be reported elsewhere but for the present

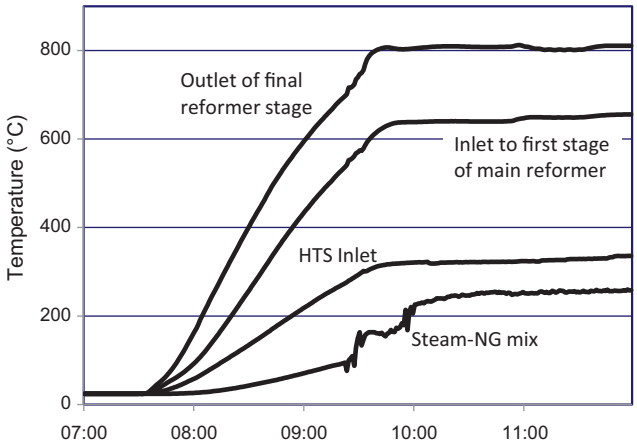

Fig. 7. Typical start-up temperature histories.

purposes we report results obtained when the catalyst was operating at about 30% of its intended effectiveness. Under these conditions, there was minor degradation in the efficiency of the process, both in terms of the heat available for recovery in the multi-stream feed-effluent exchanger and in terms of the H_2 yield. However, the intrinsic performance of the main combustor/reformer blocks was unaffected and we therefore focus on that in this paper.

4.1. Start-up

Fig. 7 shows the course of a start-up from cold. The combustion train is fired initially with hydrogen while 15 bar N_2 is introduced to the reformer side. Once the steam system is up to pressure, the N_2 is cut off and natural gas is introduced to begin making syngas – this is at 09:20 in Fig. 7, 100 min after starting up. After a further 40 min during which the syngas production rate is brought up to nominal capacity, the hydrogen start-up fuel is replaced with the operational fuel. In most cases, we used syngas product to fuel the plant – typically this was diluted 50% in N_2 in order to simulate a low-grade fuel such as might be derived from an anode off-gas or a PSA off-gas.

The complete startup is completed in less than 2.5 h, after which the plant operates very stably without need for operator intervention.

4.2. Operation

Table 1 shows a typical composition of the natural gas supplied to the laboratory.

4.2.1. 100% nominal capacity

Fig. 8 shows typical stagewise product compositions of the major reformate species for 100% nominal plant capacity, S/C = 3.67. Samples were withdrawn from the product headers for the prereformer stages and for every second reformer stage – not shown are the results for ethane which is decomposed essentially completely in the performer stages. Also shown in Fig. 8 is the progressive vitiation of the combustion air after the various combustion stages.

Table 1
Composition of natural gas (mol%).

CH_4	CO_2	N_2	C_2H_6
94.3%	2.2%	1.4%	2.1%

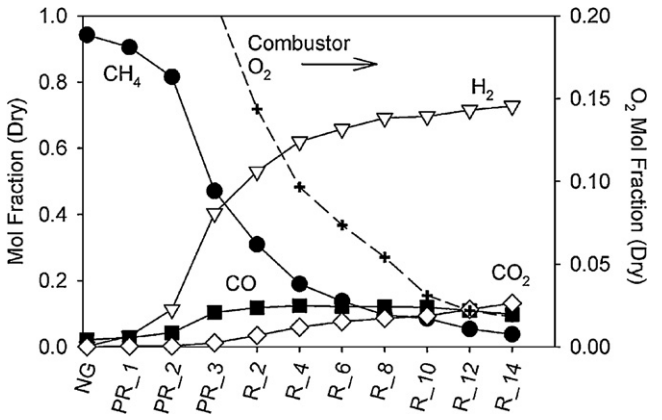

Fig. 8. Measured stagewise product evolution. The solid lines show the results for the prereformer (PR) and reformer (R) reformer stages while the dotted line shows the progressive air vitiation through the combustion beds associated with the reformer stages. Nominal plant capacity 100%.

The plant operates with a syngas outlet pressure of 13.6 bar, maintained by a back-pressure regulator. At 100% nominal production rate, the pressure drop through the entire prereformer/reformer train was 1.8 bar (prereformer inlet pressure 15.4 bar). Through the combustion train, the pressure drop was 0.31 bar.

The prereformers achieve the desired conversion of approximately 20% of the methane in the natural gas to hydrogen, after which the main reformer stages bring the conversion to about 90%. This performance can be assessed in terms of the equilibrium temperatures calculated from measured product compositions for the water-gas shift reaction (WGS: $CO + H_2O \rightleftarrows CO_2 + H_2$) and the primary steam reforming reaction (SMR-1: $CH_4 + 2H_2O \rightleftarrows CO + 3H_2$) versus measured temperatures, as in Fig. 9. Here it should be noted that reliable temperatures cannot be obtained from with the blocks and we only measure temperatures in ducts connecting blocks, with the thermocouples being surrounded with radiation shields to ensure they provide a correct gas temperature.

It is apparent in Fig. 9 that the WGS reaction reaches equilibrium in the third prereformer stage where the measured temperature is 645 °C. Beyond that, the equilibrium WGS temperature indicates that stages 2–10 have a relatively constant reaction temperature of ~740 °C. The SMR reaction does not equilibrate until about the 8th reforming stage after which the SMR and WGS equilibrium

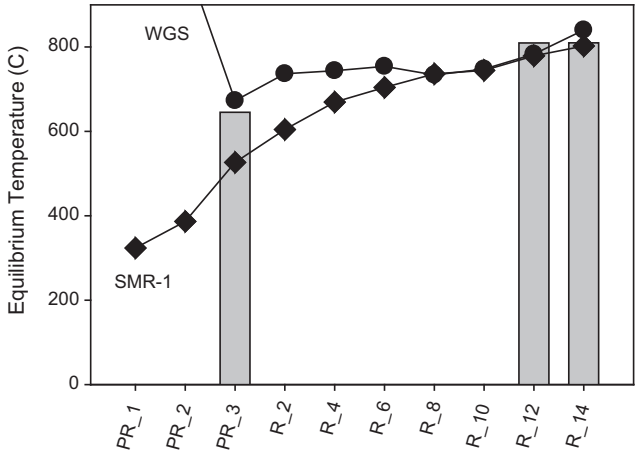

Fig. 9. Equilibrium temperatures through the reformer train. Temperatures calculated from measured gas compositions for WGS ($CO + H_2O \rightleftarrows CO_2 + H_2$) and SMR-1 ($CH_4 + 2H_2O \rightleftarrows CO + 3H_2$) reactions. The grey bars show the measured temperatures at the outlets of the accessible stages. Nominal plant capacity 100%.

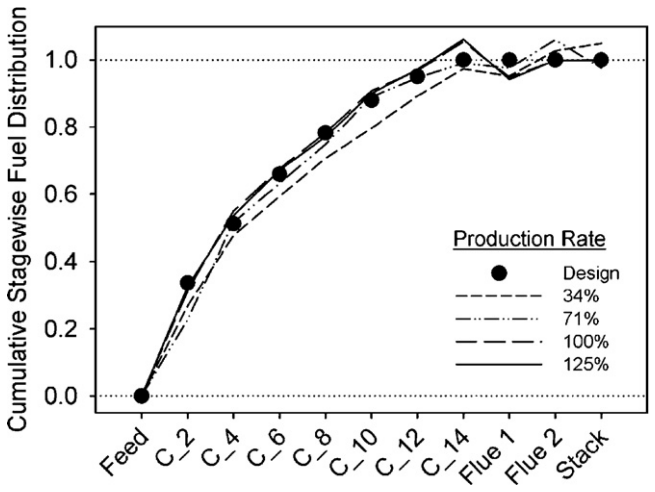

Fig. 10. Cumulative stagewise distribution of fuel at different plant production rates.

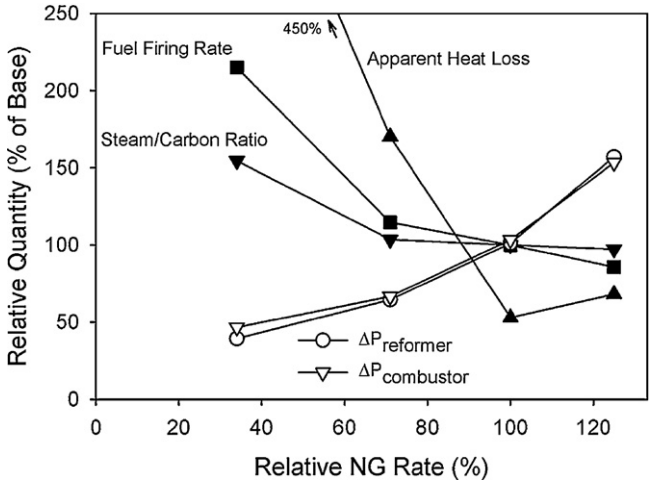

Fig. 11. Relative changes in specific heat loss (kJ kg_{NG}^{-1}), specific fuel firing rate ($(kg_{fuel}\ kg_{NG}^{-1})$ and equilibrium steam–carbon ratio as a function of plant production rate. Relative changes in overall pressure drops through the reformer and combustion trains are shown.

temperatures agree closely with each other and with the available duct measurements. The exit condition from the reformer is equilibrated at the exit temperature ~810 °C.

As discussed above, the stagewise distribution of fuel to the combustion train determines the overall temperature profile through the reactor system. The distribution in the operating plant was determined through use of a helium tracer introduced with the fuel and analysed via gas chromatography at the available sampling points. Fig. 10 shows the results (solid line) for the cumulative distribution at 100% nominal capacity, compared with the design distribution corresponding to the temperature profile in Fig. 3 – note that no fuel is introduced after stage 14. It is apparent that the fuel distribution network as implemented in the plates is faithful to the design and achieves the objective of providing autoregulated control of this very complex distribution across a wide range of operating conditions.

Table 2 shows an overview of the system energy balances obtained for 100% nominal capacity. On the reformer side the inputs are the natural gas and water streams while the outputs are the syngas and the blowdown for the steam generation system. On the combustion side, the air and fuel mixture streams are the inputs and the flue gas is the only output.

The energy balance indicates an imbalance corresponding to an apparent heat loss of 360 W, or about 5% of the combustion heat release of 6430 W. The mean value for the heat loss rate obtained in multiple runs was 650 W, which we can compare with what might be expected from a small scale process operating at 800 °C. The effective loss coefficient based on the total surface area of the box containing the plant is ~0.1 W m^{-2} K^{-1}. This corresponds to a thickness of thermal insulation (k = 0.03 W m^{-1} K^{-1} for Microtherm Super G) of the order of 0.3 m which is close to what was actually used. It is concluded that the losses are as small as can reasonably be achieved with a plant at this scale.

Another "loss" from the system is that associated with the blowdown of water from the steam generator. We feed sufficient water to ensure that the steam generator level does not drop below safe levels, with the excess water (saturated at 200 °C, 15 bar) being released without heat recovery. This surplus water also prevents the accumulation of salts in the steam generator. Although the flow of blowdown water is small in absolute terms (0.81 kg h^{-1}), it does represent about 15% of the water feed to the system and incurs a sensible heat loss of 175 W or 2.5% of the fired duty. While this is relatively small, it would be desirable to reduce this loss significantly – this would be easily accomplished at larger scale, but at the current scale, and with the objective of avoiding active control, there is room for improvement.

Direct comparison of the test results with the system design is not possible because we did not use PSA to strip hydrogen from the syngas but rather used a fraction of the actual syngas as the fuel. To compare the efficiency of the demonstration with the design performance, we assume that 80% of the hydrogen content of the syngas produced is available for export after hypothetical PSA separation, giving $\eta_{H_2} = 71.5\%$. Assuming average heat losses of 650 W gives a revised figure of 72.3% versus an expected value of 78.6% – as discussed above, the HTS reactor in our system performed poorly, leading to a ~7% loss in hydrogen yield which, if corrected, would put the plant performance very close to design. Even without these adjustments, the nominal plant production rate of 2.33 mol H_2 exported per mol NG fed remains excellent.

Further comparison with the balanced design can be made in terms of the energy available in the residual syngas after selective removal of 80% of the gross hydrogen product. The fuel that would be available for the process is calculated to be ~98% of that actually needed in the trials, confirming that the system is operating very near the design point.

4.2.2. Turndown

The system was tested from 34% to 125% of nominal capacity – the natural gas rate is simply set to the desired value and the fuel rate is adjusted to give the desired reformer outlet temperature while maintaining the air rate to give the target residual oxygen in the flue gases. As discussed above, the relative fuel distribution is essentially unchanged as the firing rate changes. No other adjustments are made and the system settles quickly (~10 min) to its new production rate.

Fig. 11 shows the principal results obtained for different feed rates of natural gas to the reformer, referred to the nominal standard value. The apparent specific heat loss (kJ kg_{NG}^{-1}) inferred from the imbalance in energy flows into and out of the system becomes much larger at lower rates although the absolute heat loss in every case remains below 1 kW. One might therefore expect that the system would demand only a small increase in the specific firing rate ($kg_{fuel}\ kg_{NG}^{-1}$) to compensate for this loss and this is clearly the case for 71% and 125% production rates. However, there is a very large increase in the required firing rate at the lowest production rate of 34%, coupled with a sharp increase in the equilibrium S/C ratio. This behaviour relates to the intensive heat integration in the system:

Table 2
Energy balances for the reformer operating at 100% capacity. The shaded boxes denote input streams.

Stream	T (°C)	Flow rate		Stream enthalpy (kJ kg^{-1})	Energy flow (kW)	Flow rate per unit NG flow				
		kmol h^{-1}	kg h^{-1}			Mass (kg kg^{-1})	Energy (kJ kg^{-1})			
Reformer										
NG	26.1	0.071	1.231	−4769	−1.63	1.00	−4770	−76243		
Water	22.6	0.308	5.550	−15850	−24.44	4.51	−71474		Δ = 17289	
Syngas	118.0	0.459	5.971	−10111	−16.77	4.85	−49043	−58954		
Blowdown	200.3	0.045	0.810	−15060	−3.39	0.66	−9911			Δ = −1047
Combustor										
Air	25.4	0.301	8.711	−14	−0.03	7.08	−88	−6317		
Fuel (mix)	28.0	0.187	3.336	−2295	−2.13	2.71	−6229		Δ = −18336	
Flue gases	118.0	0.443	12.030	−2522	−8.43	9.77	−24653	−24653		
				Imbalance	−0.36					

the relative firing rate must be increased to compensate for the relatively greater heat losses at low production rate. This results in an increased mass flow to the flue gas cooler which in turn leads to in an increase in the inlet steam quality to the boiler, thus raising more steam in the boiler, as per Eq. (1). This effect is therefore a highly nonlinear function of heat losses that are inevitably more significant at the smallest throughputs – at higher firing rates (>70%), the autoregulation capabilities of the system are clear, with the S/C ratio changing only ±3% for 25–30% variations in production rate around the design point.

The pressure drops in the combustion and reformer trains also vary with plant production rate, Fig. 10. The pressure drops at 125% of nominal capacity show a marked increase above those at 100% and provide a practical operating limit to the capacity of the plant. At lower flow rates, the pressure drops vary more or less linearly with production rate, although this is somewhat obscured by the disproportionately high firing rate and S/C ratio caused by heat losses at the lowest throughput tested.

5. Conclusions

We have demonstrated the successful operation of a standalone convective steam–methane reformer based on a multiple adiabatic catalytic bed configuration implemented using printed circuit/diffusion bonding technology. The system incorporates very high degrees of heat integration, producing relatively cold product streams and no steam export. The efficiency of the plant is correspondingly high.

Techniques to manage issues relating to excessive carbon activity that might give rise to carbon deposition or metal dusting have been incorporated into the process design and have been shown to be effective. To date, the plant has undergone >90 startups from cold without any difficulties with materials manifesting themselves. This is especially significant given the very rapid startup that would impose intolerable thermal stresses on a conventional design, Successful demonstration of this plant opens up new possibilities in the integration of process innovation and plant design and construction. The printed-circuit manufacturing technique allows very complex processes to be implemented without significant cost penalty, thus enhancing opportunities for heat integration beyond what is achievable with separate vessels, each typically performing a single unit operation and requiring interconnection via piping. Passive fluidic control can also be designed into the system to achieve a high degree of autoregulation over a wide range of turndown.

The microchannel plates at the heart of the printed-circuit technique create perfectly scalable systems, whereby the design production scale can be varied at will by varying the number of channels, e.g. by varying the plate size, the number of plates that go into a module, or the number of modules that are combined (perhaps under a common header arrangement) to create the overall plant. While we have demonstrated a system with a production rate about 4 orders of magnitude smaller than world-scale steam–methane reformer plant, there is no technical reason why this plant cannot be implemented at world scale and beyond, or at any intermediate scale, thus breaking the usual tyranny of scale in chemical process engineering.

Acknowledgements

The Heatric Division of Meggitt (UK) manufactured the heat exchanger/reactor system and funded the test program for which the authors are grateful, as they are for permission to publish. Additional support has been provided through a research grant from the Australian Research Council (DP 0985453). The efforts of Carlos Moreno, Emilie Seris and Gregory Abramowitz in construction and operation of the test facility are gratefully acknowledged.

References

[1] C.F. Cullis, D.E. Keene, D.L. Trimm, J. Catal. 19 (1970) 378–385.
[2] J.R. Rostrup-Nielsen, D.L. Trimm, J. Catal. 48 (1977) 155–165.
[3] D.L. Trimm, Catal. Today 37 (1997) 233–238.
[4] D.L. Trimm, Z.I. Önsan, Catal. Rev. – Sci. Eng. 43 (2001) 30–84.
[5] A.K. Avci, D.L. Trimm, D.L.M. Karakaya, Catal. Today 155 (2010) 66–74.
[6] A.M. Johnston, B.S. Haynes, Chemical Reactor, US Patent 7,276,214 (2007).
[7] E.L.C. Seris, G. Abramowitz, A.M. Johnston, B.S. Haynes, Chem. Eng. J. 135S (2008) 9–16.
[8] E.L.C. Seris, G. Abramowitz, A.M. Johnston, B.S. Haynes, Chem. Eng. Res. Des. 83 (2005) 619–625.
[9] J.R. Rostrup-Nielsen, Steam reforming, in: G. Ertl, H. Knözinger, F. Schüth, J. Weitkamp (Eds.), Handbook of Heterogeneous Catalysis, 2nd ed., Wiley-VCH, Weinheim, 2008, pp. 2882–2905.
[10] M. Zanfir, A. Gavriilidis, Chem. Eng. Sci. 58 (2003) 3947–3960.
[11] A.L.Y. Tonkovich, B. Yang, S.T. Perry, S.P. Fitzgerald, Y. Wang, Catal. Today 120 (2007) 21–29.
[12] L. Ma, D.L. Trimm, Appl. Catal. A 138 (1996) 265–273.
[13] P. Ferreira-Aparicio, M.J. Benito, J.L. Sanz, Catal. Rev. 47 (2005) 491–588.
[14] M.S. Mettler, G.D. Stefanidis, D.G. Vlachos, Ind. Eng. Chem. Res. 49 (2010) 10942–10955.
[15] E. Kikuchi, Catal. Today 56 (2000) 97–101.
[16] A.M. Johnston, Reforming Apparatus and Method, US Patent Application 2008/0244975 (2008).
[17] J.F. Contadini, C.V. Diniz, D. Sperling, R.M. Moore, Hydrogen Production Plants: Emissions and Thermal Efficiency Analysis, Institute of Transportation Studies, University of California, 2000.
[18] A.P. Simpson, A.E. Lutz, Int. J. Hydrogen Energy 32 (2007) 4811–4820.
[19] P. Häussinger, R. Lohmüller, A.M. Watson, Hydrogen, in: Ullmann's Encyclopedia of Industrial Chemistry, Wiley-VCH Verlag GmbH & Co., Weinheim, 2007.